Simulating the MIMO Outdoor-to-Indoor Propagation Environment

M Newton and D Kitchener
Nortel Networks

Abstract: The convergence of voice and data services over the wireless medium means that cellular operators are increasingly interested in characterising the Outdoor-to-Indoor channel which is the typical scenario where data services will be used. The combined requirement of higher data rates and lower BERs for the data services mean that a comprehensive understanding of the Outdoor-to-Indoor propagation environment is required so that it can be optimally exploited. For example there is currently a lot of interest in using Multiple-Input/Multiple-Output (MIMO) systems to provide higher capacities/data rates by exploiting different 'spatial modes' of multipath rich environments. The aim of this paper is to present a novel technique of modelling the MIMO Outdoor-to-Indoor channel.

1. Introduction

This paper describes a statistical channel model for an outdoor-to-indoor Multiple-Input/ Multiple-Output (MIMO) link in either an inner city urban or suburban residential environment. The model has been developed initially for co-polarised, spatially separated antennas at both the Basestation (Node B) and the User Equipment (UE) ends of the link. For the given environment the Node B antenna is assumed to be clear of local scatterers, and therefore these are located only about the building in which the UE is located. The model includes the angle spread of the multipath for both ends of the link, which enables calculation of the MIMO channel matrix. The model also includes temporal fading such that time variation of the channel is accurately modelled.

2. Simulation Overview

The Outdoor to Indoor channel model uses the following methodology:

- Randomly select an average Channel Impulse Response (CIR) from a set of measured profiles for either an urban or suburban environment.
- Attribute angles-of-arrival (as seen from the Node B) to each resolvable multipath component (200ns resolution) using measured angle spread statistics obtained in Central London.
- Determine the geometrical position of scatterers using the angle and delay of each multipath component as well as the range between the Node B and the UE. This is done using the equations of an ellipse where the Node B and UE antennas are at the foci.
- A Gaussian weighting function about a randomly selected preferred direction is applied to the outdoor local scatter powers to emulate the angularly dependent spatial filtering that occurs at the outdoor-to-indoor interface.
- A lognormal shadowing component is applied to each outdoor local scatterer power to emulate the variation in mean signal power that occurs at the outdoor-to-indoor interface.
- Use the indoor-to-indoor statistical channel model [1] to generate the delay, amplitude, phase and angle-of-arrival (AoA) information for all of the non-resolvable multipath, as seen at the UE, for each resolvable ray of the selected CIR.
- The channel generated by the indoor-to-indoor model represents the channel from the Node B reference element to the UE reference element.
- Indoor multipath are then associated with outdoor local scatterers so as to give angle spread at seen at the Node B.
- The far field assumption is used to determine the phase shift for each multipath to spatially separated Node B or UE elements.
    - Phase shifts at the UE are determined using the AoA generated by the indoor-to-indoor model.
    - Phase shifts at the Node B are generated by using the AoA (as seen from the Node B) due to the outdoor scatterer locations.
- A random Doppler shift component between ±4Hz is applied to a subset of the multipath components (on the reference channel) to simulate temporal fading.

3. Determining the Channel Impulse Response as seen at the Subscriber

To provide realistic channels, CIRs are randomly selected from a set of measured profiles, using either an urban or suburban dataset depending on the environment to be simulated. The selected CIR defines the number of resolvable multipath, as well as the power ratio and the relative delay offsets between them. Next AoA information (as seen at the Node B) is attributed to each multipath using a set of measured CDFs of angle-window for different power thresholds. The technique used to determine an AoA for a multipath is explained in Figure 1.

- Resolvable Angles-of-Arrival (as seen from the Node B)

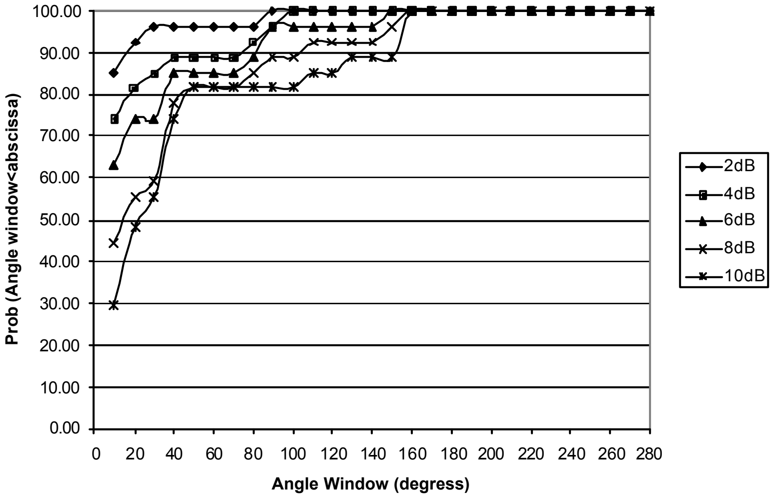

1) Determine which cdf to use depending on power of tap. Is tap power <=-2dB, -4dB, -6dB, -8dB or –10dB.
2) Generate U(0,1) number
3) When appropriate cdf is identified, then the closest angle bin for the given U(0,1) probability is determined.
4) Then a random angle within the identified angle range is generated.
5) This is repeated for all of the wideband taps above the set power threshold.
6) Thereby Angles-of-Arrival are attributed to each outdoor multipath component depending on their powers.

Note: U(0,1) denotes a random number between 0 and 1 drawn from a uniform distribution.

Figure 1. **Method of attributing AoA to multipath**

-Resolvable Scatterer Locations

Once we have delay and AoA information for each multipath then we can derive the geometrical positions of the scatterers that caused them by assuming that the Node B and UE are the foci of an ellipse (see Figure 2 for an example).

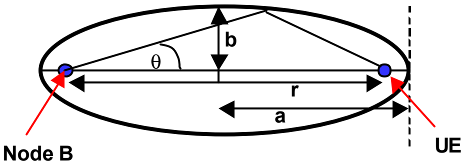

$$a = \frac{r + ct}{2} \qquad e = \frac{\sqrt{a^2 - b^2}}{a}$$

$$b = \sqrt{a^2 - \left(\frac{r^2}{2}\right)} \qquad \text{radial dist} = \frac{a\left(1 - e^2\right)}{1 - e\cos q}$$

where $c = 3 * 10^8$
where t = excess delay

x coordinate = radial dist * cosθ
y coordinate = radial dist * sinθ

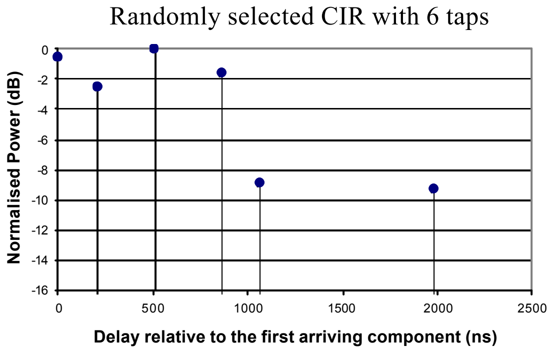

Angles (°)	Delays (ns)	Powers (dB)	x-coord (m)	y-coord (m)
3.1340	508	0	1064.1	58.265
0	0	-0.6381	1000	0
-3.2465	863.6	-1.6465	1120.8	-63.574
-2.5793	203.2	-2.5462	1012.6	-45.616
-28.5802	1066.8	-8.9161	737.77	-401.92
-4.4760	1981.2	-9.3001	1286.6	-100.72

Figure 2. **Example of method used to determine the geometrical locations of resolvable scatterers**

Having determined the spatial positions of the resolvable outdoor scatterers we can now apply a combination of a log-normal variation on the mean power and an angular filtering effect to determine which of the outdoor scatterers are seen as significant components in the indoor environment. The assumption is made that the building acts as a spatial filter. Therefore depending upon where the UE is located within the building there may be a preferred AoA (i.e. minimum penetration loss) with increased attenuation as the multipath AoA deviates from this.

The combination of the log-normal variation of the mean and the angular weighting function were optimised such that their combined effect was to provide a statistical reduction in the number of resolvable taps at the outdoor-to-indoor interface that was consistent to that observed in measurements.

Now that the powers and delays of each resolvable multipath for the indoor environment are known, the indoor-to-indoor model as proposed by Quentin Spencer et al [1] can be used to generate the amplitudes, delays, phases and AoA for all the non-resolvable components (i.e. components that have a delay separation <200ns) as seen at the UE reference element. The model works at two levels, clusters and rays. A ray is a resolvable component that has associated amplitude, phase, delay and AoA properties. A cluster is a group of rays, which are clustered about a common mean AoA and are used to represent the angular concentration of components that occur with reflections or dominant entry routes such as windows or doorways. Figure 3 shows a graphical representation of the Channel Impulse Response (CIR) as formed by the indoor-to-indoor channel model. It shows that rays are grouped in clusters, and that the power of a given ray is dependent on both the delay of a ray within a cluster and the delay at which the cluster of interest started.

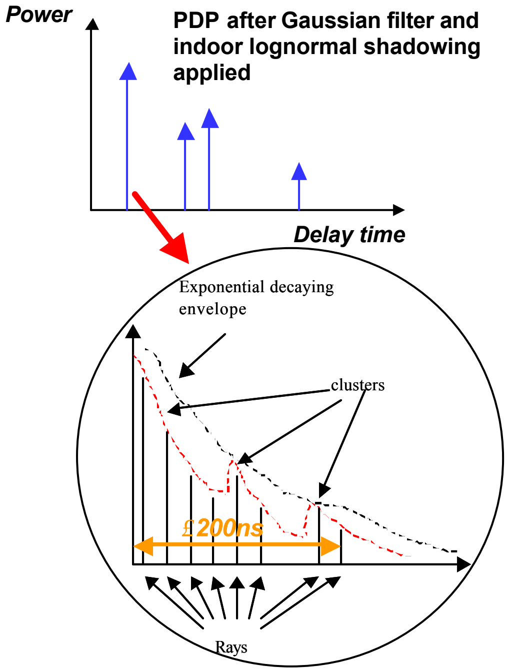

Equation 1. $$P(T_l / T_{l-1}) = \Lambda \exp[-\Lambda(T_l - T_{l-1})]$$

Equation 2. $$P(t_{kl} / t_{(k-1)l}) = l \exp[-l(t_{kl} - t_{(k-1)l})]$$

Where l denotes cluster and k represents the ray arrivals within a cluster.

$$\frac{1}{\Lambda} = 16.8ns \longleftarrow$$ ***Cluster arrival rate***

$$\frac{1}{l} = 5.1ns \longleftarrow$$ ***Ray arrival rate***

Figure 3 **Generating non-resolvable components for each resolvable wideband tap**

- *Non-resolvable Delays*

First the cluster arrival times (T_l) are determined using the conditional Poisson function given in equation 1. The first cluster arrival time T_0 is set equal to 0 to correspond to having a normalised delay of zero. Once the cluster arrival times have been determined then the ray arrival times (τ_{kl}) are generated by using another conditional Poisson function (see equation 2). The cluster and ray arrival rates shown here were determined empirically.

- *Non-resolvable Amplitudes*

Once the cluster and ray arrival times are determined then the mean powers can be attributed to the rays by using the double exponential decay relationship as shown in equation 3.

Equation 3. $$\overline{b^2_{kl}} = \overline{b^2(0,0)}\, e^{\frac{-T_l}{\Gamma}} e^{\frac{-t_{kl}}{g}}$$

$$\Gamma = 33.6ns \longleftarrow$$ ***Cluster arrival decay time constant***

$$g = 28.6ns \longleftarrow$$ ***Ray arrival decay time constant***

Where β_{kl} is the amplitude of the kth ray of the lth cluster and $\overline{b^2(0,0)}$ is the average power of the first arrival of the first cluster. The determined mean powers ($\overline{b^2_{kl}}$) are then used as means in a Rayleigh distribution to generate ray amplitudes.

- *Non-resolvable Angles-of-Arrival*

In the model used each cluster was attributed a random U(0,360) mean cluster angle. The rays AoAs within a cluster are modelled by a Laplacian distribution with a given mean (μ) and standard deviation (σ).

- *Non-resolvable Phases*

The model attributes random phases to rays using a U(0,2π) distribution.

- *CIRs at other Subscriber Elements*

Once the channel impulse characteristics for the reference element have been generated we want to determine the channel impulse response as viewed from spatially separated elements. This can be achieved, by assuming that the scatterers are sufficiently far away that we see a plane wave response across the antenna aperture and hence we can far field transform the phases from the reference element to all the other array elements.

4 Determining the Channel Impulse Response as seen at the Basestation

Once having determined the CIR at the UE end it is necessary to map these characteristics back to the reference element at the Node B end. If the uplink (UE to Node B) frequency and downlink (Node B to UE) frequency are the same then this task is relatively easy, as all propagation parameters apart from AoA are the same as viewed at the UE reference element. However if uplink and downlink frequencies are different then we need to provide a method to be able to map the phases as seen at the UE (at the downlink frequency) to the phases as seen at the Node B (at the uplink frequency). Therefore when configuring the model to cope with both up and downlink frequencies the model must provide a method to map between the random ray phases as assigned by the indoor-to-indoor model and ray phases as dictated by each ray's path length.

- *Phases*

The difference between the randomly attributed ray phases and the path length associated phases, as calculated at the downlink frequency, is taken to be the 'phase offset'.

Equation 4.

$$\text{Phase Offset}_{\text{i}} = f_i - t_i c k_{downlink} \qquad \text{k}_{\text{downlink}} = \frac{2p}{l_{downlink}}$$

Speed of Light

Ray index number

Ray phases as seen at subscriber reference element at downlink frequency.

Ray delays as seen at subscriber reference element

The 'phase offset' physically relates to the random phase perturbations that occur within the transmission environment to mean that the phase predicted for a given multipath delay (i.e. path length) can differ to that which is actually observed. Effects such as propagation through trees, reflections and re-transmissions can cause these differences. Once having determined the 'phase offset', and by assuming that it remains the same for the uplink frequency (which is a valid assumption when considering that the properties of the materials over the 60MHz frequency difference will remain constant), then the phases as seen at any uplink frequency can be determined using equation 5.

Equation 5. $Phase(at\ uplink\ frequency)_i = t_i c k_{uplink} + PhaseOffset_i$

5 Temporally Evolving the Channel

Temporal variations in the indoor channel are typically caused by events, such as people moving past doorways, windows etc. This means that typically the phases that are perturbed come from a relatively limited angular spread. Therefore to impose temporal fading in the outdoor-to-indoor model, all the rays within clusters that have nominally the same AoA (as seen at the UE end) have their phases rotated in a manner consistent with a specified Doppler frequency.

6 Summary

A novel method of modelling the MIMO outdoor-to-indoor environment, which has been parametised and validated using extensive data sets of empirically measured results, has been presented.

References.

[1] 'A Statistical Model for Angle-of-Arrival in Indoor Multipath Propagation', Quentin Spencer, Michael Rice, Brian Jeffs and Michael Jensen, IEE document No: 0-7803-3659-3/97, 1997